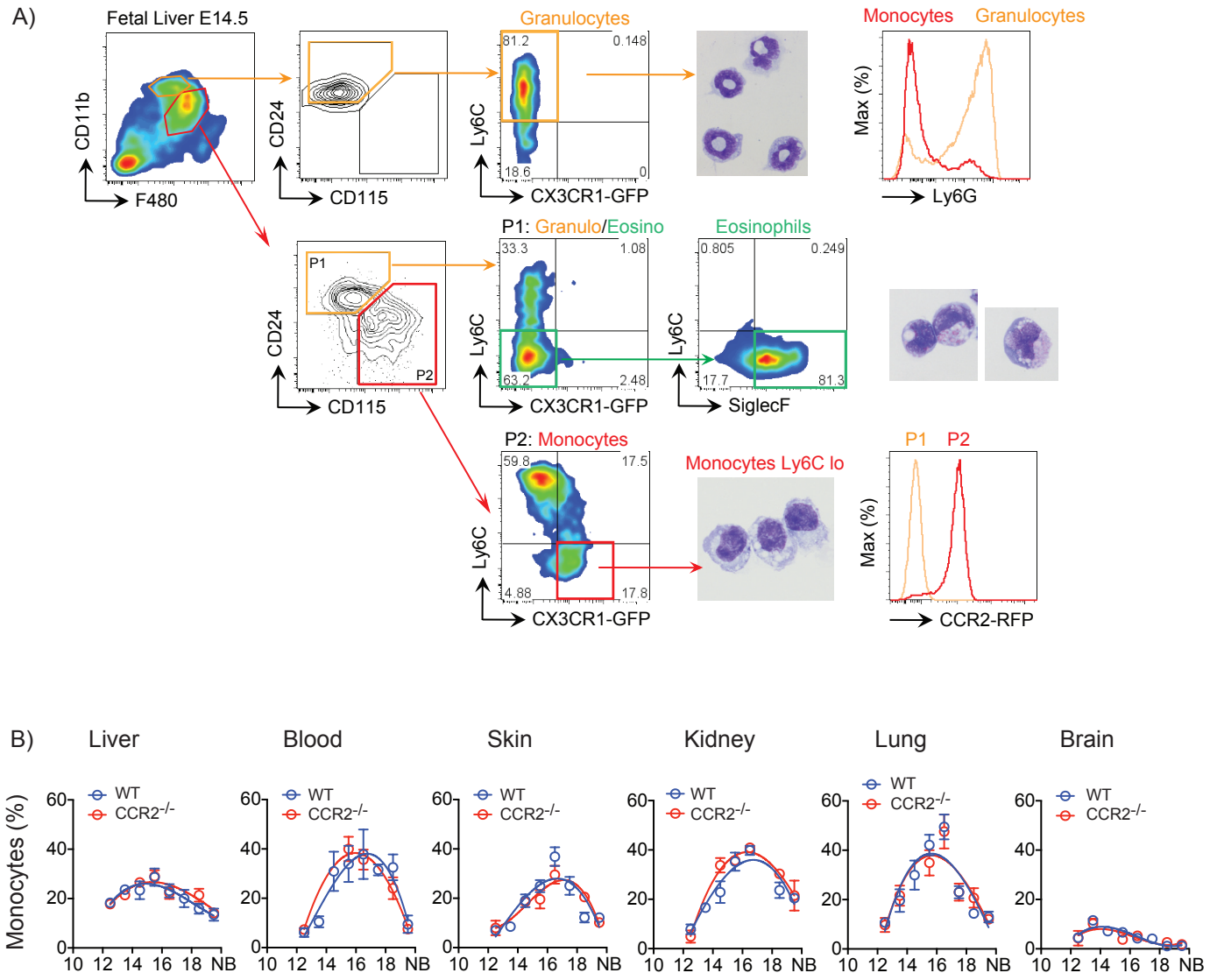

Figure S1: Fetal monocytes express CCR2 but their egress from the fetal liver and tissue seeding is CCR2 independent. *Related to Figure 1*

(**A**) Flow cytometry analysis of E14.5 FL from (doublet$^-$DAPI$^-$CD45$^+$ cells) CX3CR1-GFP and CCR2-RFP embryos. Granulocytes are CD11b^{++}F480$^-$CD24$^+$CD115$^-$ cells (yellow gate). They appear Ly6C^{int} and CX3CR1$^-$ and Ly6G$^+$. GIEMSA staining highlights their typical polymorphonuclear morphology. Other cells, CD24$^+$CD115$^-$Ly6C^{int}CX3CR1$^-$ granulocytes and CD24$^+$CD115$^-$F480$^+$Ly6C$^-$SiglecF$^+$ eosinophils (green gate) are also identified in the CD11b$^+$ F480^{lo} gate. Typical eosin$^+$ granules are highlighted by GIEMSA staining.
Monocytes are CD11b^{hi}F480^{lo}CD24^{lo}CD115$^+$ cells (red gate). Two populations appear: Ly6C$^+$ or Ly6C$^-$ and CX3CR1$^+$. Ly6C^{lo} monocytes possess more cytoplasm and granules than Ly6C$^+$ monocytes by GIEMSA staining. Fetal monocytes are CCR2$^+$ compared to granulocytes in CCR2-RFP embryos. Data are representative of two independent experiments. (**B**) Relative numbers of fetal monocytes (doublet$^-$DAPI$^-$CD45$^+$CD11b$^+$F480$^+$CD64$^+$Ly6C$^+$) were measured by flow cytometry every other day in WT or CCR2$^{-/-}$ mice. (n=5-10 from two litters of each group, bars represent mean +/- SEM).

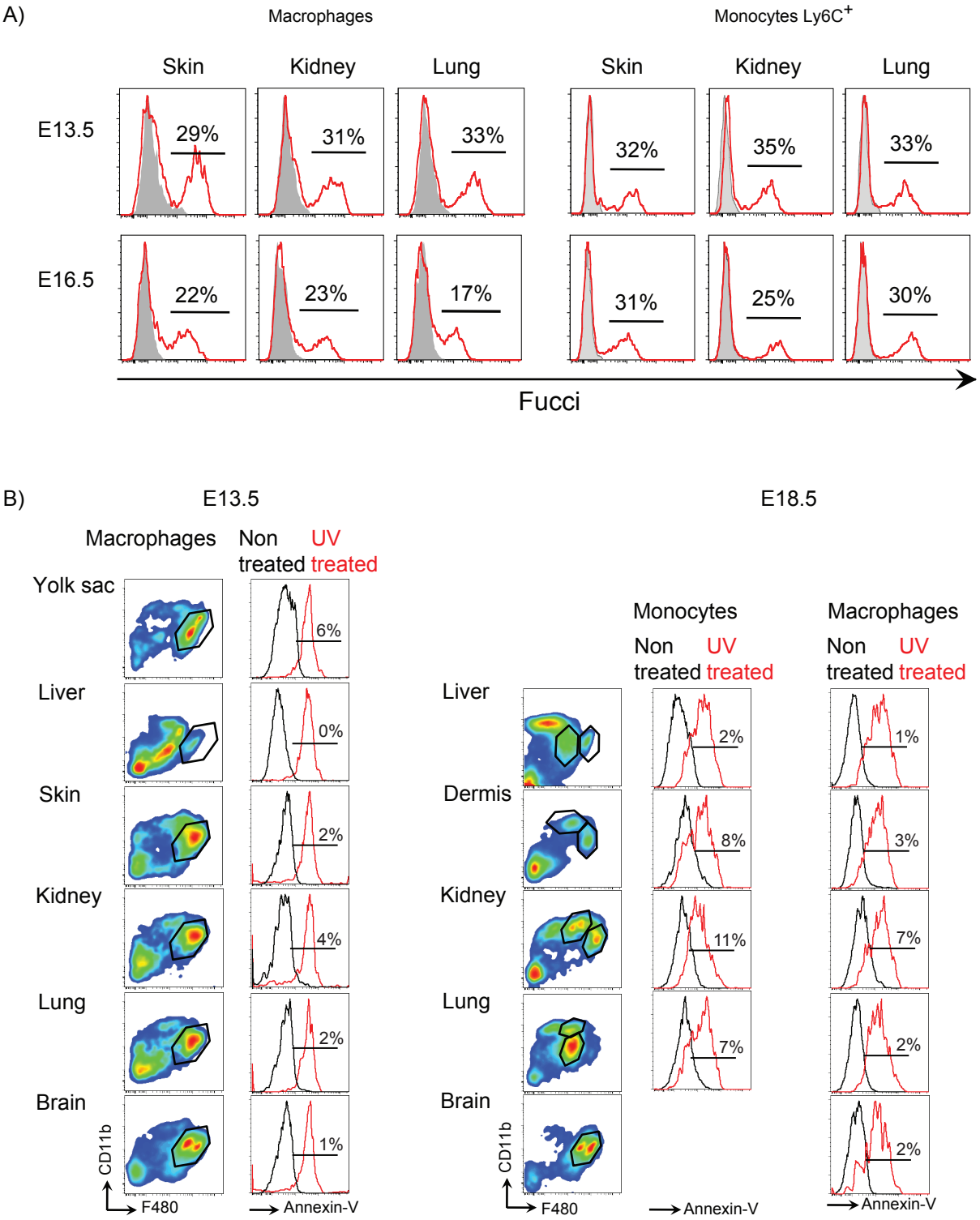

Figure S2: Fetal monocytes and macrophages proliferate in tissues and do not exhibit signs of apoptosis.
Related to Figure1 and 2

(A) Flow cytometry analysis of E13.5 and E16.5 Fucci-reporter embryos gated on doublet$^-$DAPI$^-$CD45$^+$ cells. Relative numbers of Fucci$^+$ monocytes and macrophages, gated as in *Figure 1*, are shown.
(three independent experiments).
(B) Tissues from E13.5 or E18.5 WT embryos were analyzed by flow cytometry following Annexin-V labelling. Relative numbers of apoptotic monocytes and macrophages, gated as in *Figure 1*, are shown.
One representative embryo from 3 to 5 is shown (two independent experiments).

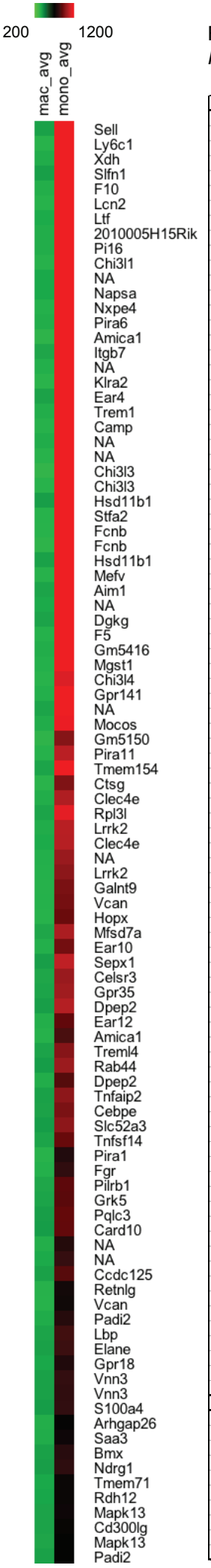

Figure S3A: List of genes expressed by fetal monocytes and not by macrophages. *Related to Figure 3*.

	Symbol	mac_avg	mono_avg
1	Sell	190.827	9125.610
2	Ly6c1	146.869	6767.368
3	Xdh	168.430	5228.261
4	Slfn1	195.201	4675.875
5	F10	160.193	3776.404
6	Lcn2	148.956	3407.892
7	Ltf	171.603	3730.278
8	2010005H15Rik	161.706	3246.730
9	Pi16	163.593	2891.694
10	Chi3l1	149.799	2526.519
11	NA	175.076	2438.127
12	Napsa	175.721	2171.744
13	Nxpe4	155.720	1863.950
14	Pira6	165.112	1936.632
15	Amica1	135.750	1519.459
16	Itgb7	181.945	2015.592
17	NA	157.869	1723.753
18	Klra2	141.451	1495.316
19	Ear4	189.321	1983.292
20	Trem1	163.908	1666.857
21	Camp	151.329	1499.494
22	NA	167.910	1644.467
23	NA	143.551	1377.736
24	Chi3l3	123.961	1132.449
25	Chi3l3	143.457	1283.186
26	Hsd11b1	196.914	1698.839
27	Stfa2	149.412	1285.698
28	Fcnb	145.611	1211.880
29	Fcnb	136.556	1135.400
30	Hsd11b1	190.825	1577.937
31	Mefv	150.246	1229.919
32	Aim1	185.772	1443.263
33	NA	173.593	1334.073
34	Dgkg	186.526	1384.753
35	F5	152.176	1113.985
36	Gm5416	164.138	1198.966
37	Mgst1	155.856	1119.732
38	Chi3l4	144.153	1030.158
39	Gpr141	158.160	1129.752
40	NA	185.223	1220.807
41	Mocos	168.399	1073.962
42	Gm5150	132.339	832.314
43	Pira11	154.788	956.678
44	Tmem154	185.242	1106.063
45	Ctsg	139.641	820.052
46	Clec4e	161.890	933.216
47	Rpl3l	184.459	1054.091
48	Lrrk2	168.692	952.924
49	Clec4e	171.618	951.758
50	NA	159.268	878.246
51	Lrrk2	155.583	848.871
52	Galnt9	153.620	810.165
53	Vcan	152.060	801.017
54	Hopx	148.605	774.670
55	Mfsd7a	179.992	921.676
56	Ear10	158.742	790.701
57	Sepx1	197.303	970.717
58	Celsr3	180.225	879.825
59	Gpr35	184.380	895.983
60	Dpep2	196.317	945.783
61	Ear12	160.390	756.514
62	Amica1	153.993	703.220
63	Treml4	186.539	837.337
64	Rab44	198.860	884.286
65	Dpep2	164.133	726.976
66	Tnfaip2	193.893	855.468
67	Cebpe	189.449	811.582
68	Slc52a3	199.829	852.651
69	Tnfsf14	184.368	770.984
70	Pira1	145.476	602.409
71	Fgr	157.222	646.578
72	Pilrb1	181.066	744.327
73	Grk5	184.546	737.865
74	Pqlc3	196.280	760.970
75	Card10	198.154	758.053
76	NA	160.583	613.263
77	NA	173.362	659.633
78	Ccdc125	192.175	729.409
79	Retnlg	151.323	562.156
80	Vcan	149.217	554.294
81	Padi2	166.961	619.834
82	Lbp	185.524	687.683
83	Elane	193.932	672.707
84	Gpr18	176.137	600.961
85	Vnn3	193.755	655.686
86	Vnn3	191.305	646.366
87	S100a4	198.450	650.521
88	Arhgap26	160.544	523.433
89	Saa3	168.607	547.551
90	Bmx	192.389	622.969
91	Ndrg1	197.864	640.050
92	Tmem71	173.925	543.167
93	Rdh12	178.497	541.256
94	Mapk13	186.036	547.784
95	Cd300lg	187.334	532.416
96	Mapk13	183.463	519.159
97	Padi2	192.932	511.256

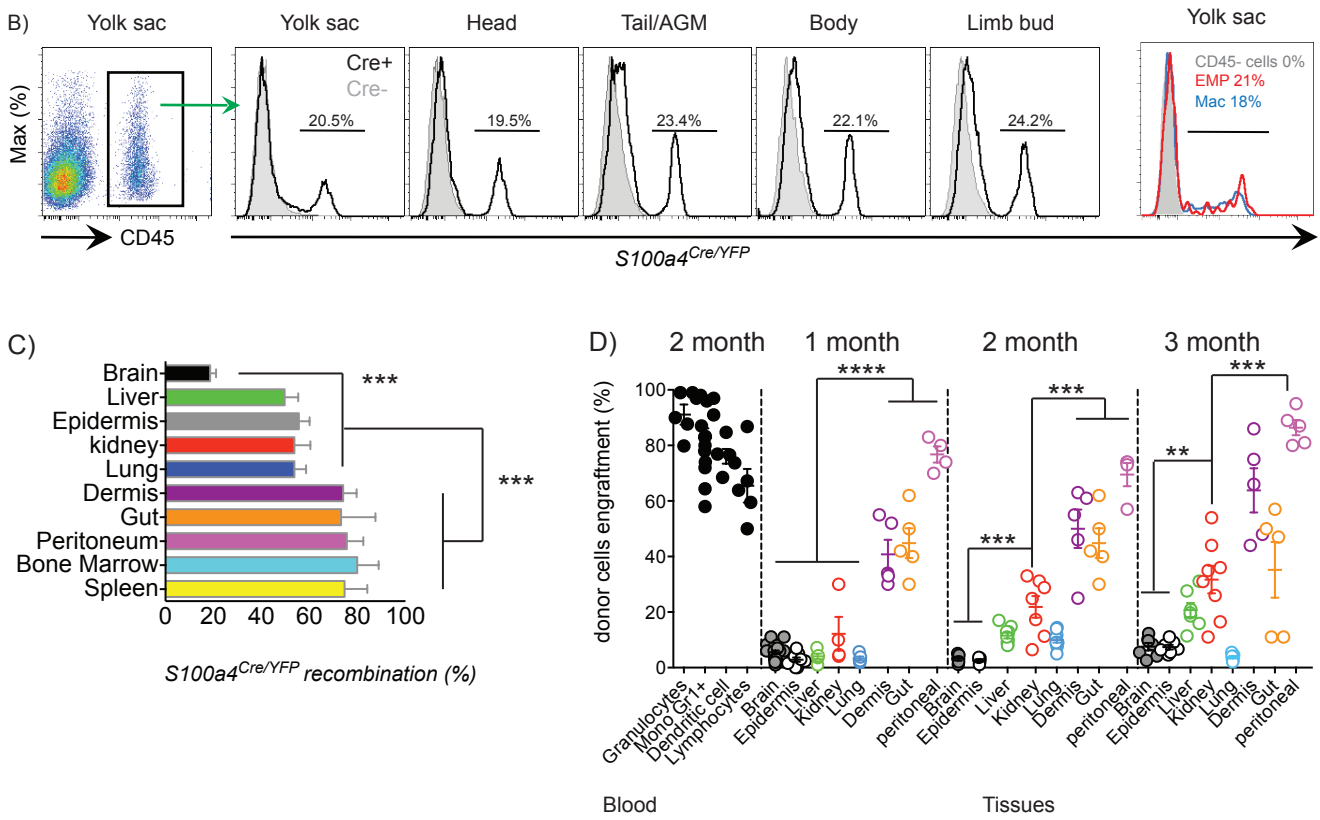

Figure S3: *S100a4*$^{Cre/YFP}$ recombination in embryos, adult tissue macrophages and newborn bone marrow transplantation assay. *Related to Figure 3.*

(**A**) Skin/dermis monocytes and macrophages were sorted and mRNA was extracted and processed for gene array analysis. Hierarchical clustering of monocytes and macrophages (See also Supplemental Methods) from fetal dermis and epidermis at E16.5 and E17.5 were used to select genes only expressed in fetal monocytes and not in macrophages. Differentially expressed genes (DEGs) were selected by using Linear Models for Microarray Data (Limma) and an FDR cut-off of 0.05. The first 97 genes expressed exclusively by fetal monocytes are shown. *S100a4* is highlighted in red in the list.
(**B**) *S100a4*$^{Cre/YFP}$ embryos were collected at E10.5 and analyzed by flow cytometry. Relative numbers of YFP^{+} cells within CD45^{+} leukocytes from different tissues are presented. (Right) Relative numbers of YFP^{+} cells in YS EMPs (Red) and YS macrophages (Blue) are highlighted compared to CD45^{-} cells (Grey). One embryo representative from two litters is shown.
(**C**) Graph shows YFP^{+} recombination percentage of tissue-resident macrophages in *S100a4*$^{Cre/YFP}$ mice (5 week-old) analyzed by flow cytometry. Bars represent mean +/- SEM from three pooled experiments. The gating strategy for each population was described previously (Ginhoux et al., 2010).
(**D**) Newborn CD45.2^{+} mice were sub-lethally irradiated and reconstituted with bone marrow cells from adult CD45.1^{+} mice. The extent of blood leucocyte and tissue macrophage chimerism was measured by flow cytometry at one, two or three months after transplantation. Each dot represents a single mouse. Throughout the figure ANOVA, *p < 0.05; ** p < 0.01; ***p < 0.001.

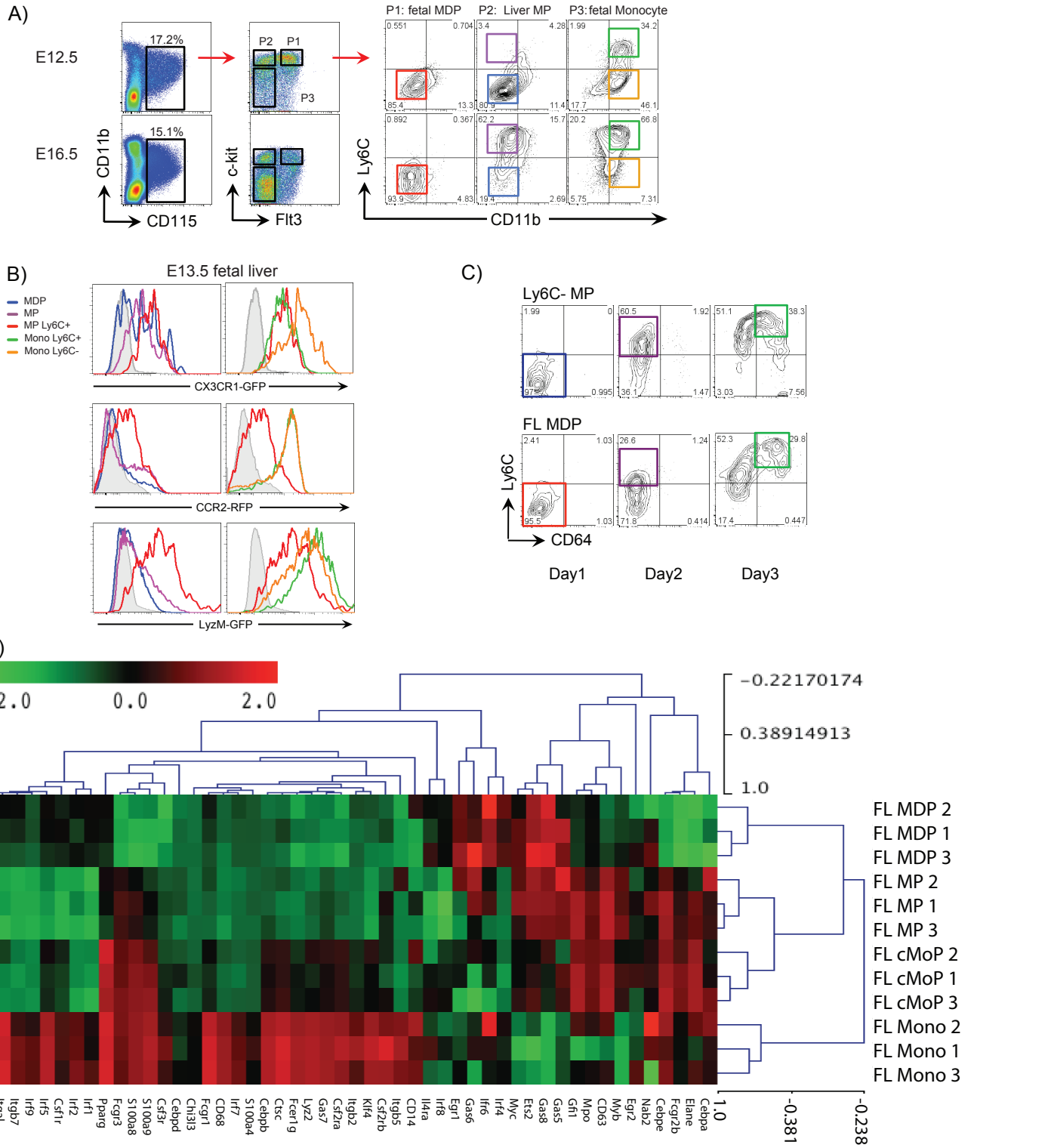

Figure S4: Fetal liver myeloid progenitor phenotype, in vitro potential anf gene array analysis.
Related to Figure 4

(**A**) FL of E12.5 or E16.5 embryos were analyzed by flow cytometry (doublet$^-$DAPI$^-$CD45$^+$ cells). Gating strategy depicts FL MDP (red), FL MP (blue), FL cMoP (purple) and FL monocytes (green) as in *Figure 4A*.
FL MP population progressively declines after E16.5. (**B**) FL myeloid progenitors (as in A) were analysed by in E14.5 CX3CR1-GFP, CCR2-RFP or Lyzozyme-GFP embryos . (**C**) In vitro culture of FL MDP and FL MP in complete medium supplemented with 10 ng/ml CSF-1. Data are representative of three independent experiments.
(**D**) Heatmap of myeloid genes and transcription factors involved in monopoiesis, adapted from (Friedman, 2002) and (Molawi and Sieweke, 2013). Results show myeloid enrichment in cMoP and monocytes.
(**E**) (Next page) DEG for each myeloid progenitor reveal lymphoid and erythroid gene expression patterns in FL MDP and FL MP respectively. (Left) General heatmap showing DEG for each population (FL and BM). (Middle) DEG list for FL MDP, FL MP and fetal monocytes (Right). Lymphoid genes (red) and erythroid/megakaryocyte genes (blue) for each population are depicted. FL cMoP do not possess specific DEG as they share gene expression patterns with both early progenitors (FL MDP or FL MP) and fetal monocytes.
Note that fetal monocytes do not express lymphoid or erythroid genes. See *Supplemental Tables and Methods.*

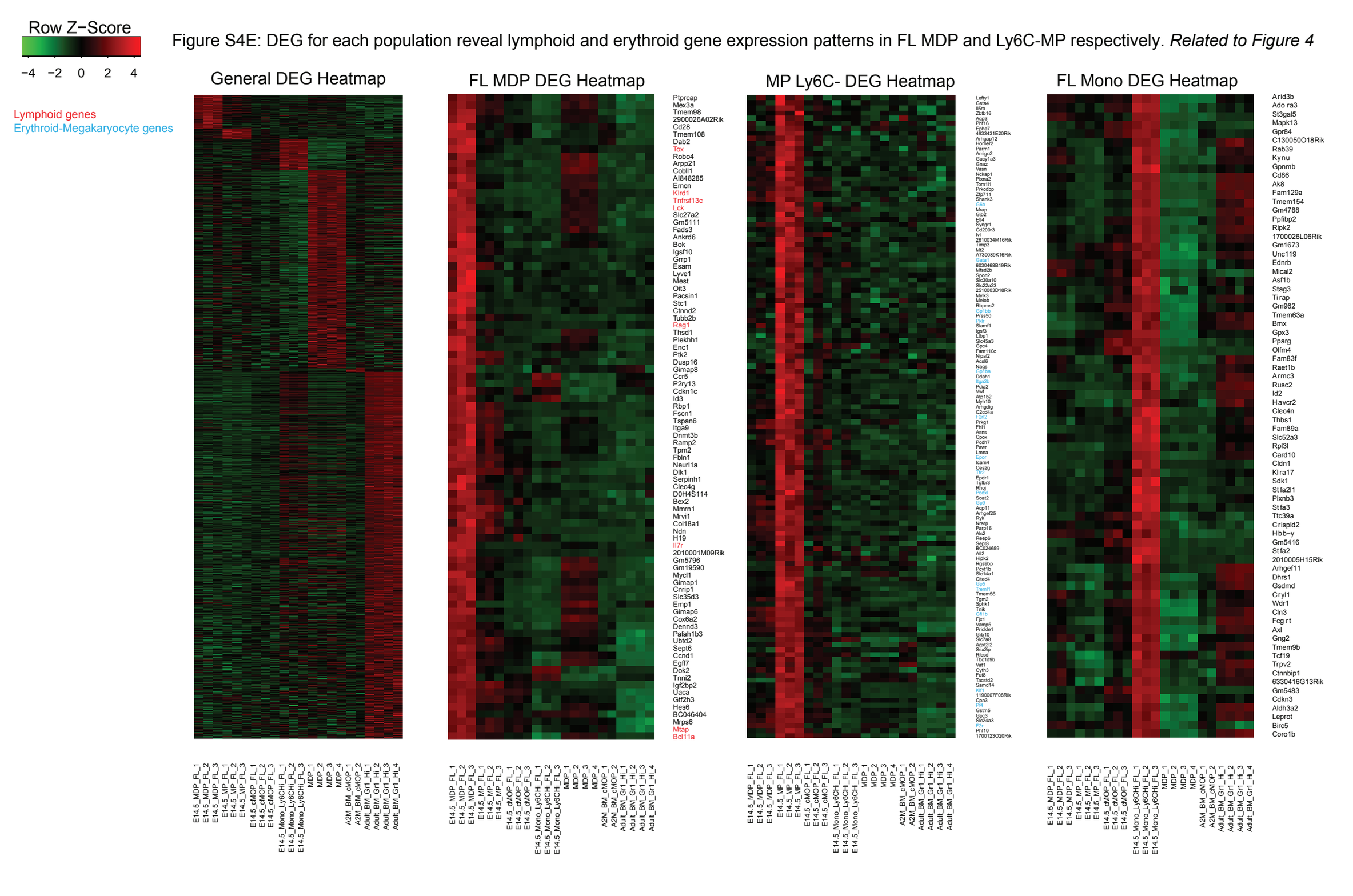
Row Z−Score
−4 −2 0 2 4
Figure S4E: DEG for each population reveal lymphoid and erythroid gene expression patterns in FL MDP and Ly6C-MP respectively. *Related to Figure 4*
Lymphoid genes
Erythroid-Megakaryocyte genes
General DEG Heatmap
FL MDP DEG Heatmap
MP Ly6C- DEG Heatmap
FL Mono DEG Heatmap
Ptprcap
Mex3a
Tmem98
2900026A02Rik
Cd28
Tmem108
Dab2
Tox
Robo4
Arpp21
Cobll1
AI848285
Emcn
Klrd1
Tnfrsf13c
Lck
Slc27a2
Gm5111
Fads3
Ankrd6
Bok
Igsf10
Grrp1
Esam
Lyve1
Mest
Olt3
Pacsin1
Stc1
Ctnnd2
Tubb2b
Rag1
Thsd1
Plekhh1
Enc1
Ptk2
Dusp16
Gimap8
Ccr5
P2ry13
Cdkn1c
Id3
Rbp1
Fscn1
Tspan6
Itga9
Dnmt3b
Ramp2
Tpm2
Fbln1
Neurl1a
Dlk1
Serpinh1
Clec4g
D0H4S114
Bex2
Mmrn1
Mrvi1
Col18a1
Ndn
H19
Il7r
2010001M09Rik
Gm5796
Gm19590
Mycl1
Gimap1
Cnrip1
Slc35d3
Emp1
Gimap6
Cox6a2
Dennd3
Pafah1b3
Ubtd2
Sept6
Ccnd1
Eqfl7
Dok2
Tnni2
Igf2bp2
Uaca
Gtf2h3
Hes6
BC046404
Mrps6
Mtap
Bcl11a
Lefty1
Gsta4
Il5ra
Zbtb16
Aqp3
Phf16
Epha7
4933431E20Rik
Arhgap12
Homer2
Parm1
Amigo2
Gucy1a3
Gnaz
Vasn
Nckap1
Plxna2
Tom1l1
Prkcdbp
Zfp711
Shank3
G6b
Mrap
Gjb2
Ell4
Syngr1
Cd200r3
Ivl
2610034M16Rik
Timp3
Mtl2
A730089K16Rik
Gata1
6030468B19Rik
Mfsd2b
Spon2
Slc30a10
Slc22a23
2510003D18Rik
Mylk3
Meiob
Rbpms2
Gp1bb
Prss50
Pf4
Slamf1
Igsf3
Lbp1
Slc45a3
Gpc4
Fam110c
Nipal2
Acsl6
Nags
Gp1ba
Ddah1
Itga2b
Pdia2
Vwf
Atp1b2
Myh10
Arhgdig
C2cd4a
F2rl2
Prkg1
Fhl1
Asns
Cpox
Pcdh7
Pawr
Lmna
Epor
Icam4
Ces2g
Tfr2
Epdr1
Tgfbr3
Rhoj
Podxl
Soat2
Gp9
Aqp11
Arhgef25
Ryk
Nrarp
Parp16
Als2
Reep6
Sept8
BC024659
Atl2
Hipk2
Rgs9bp
Pcyt1b
Slc14a1
Cited4
Gp5
Trem1
Tmem56
Tgm2
Sphk1
Tnik
Olr1b
Fjx1
Vamp5
Prickle1
Grb10
Slc7a8
Agxt2l2
Ssx2ip
Rtkn2
Tbc1d9b
Vat1
Cyth3
Fut8
Tacstd2
Samd14
Klf1
1190007F08Rik
Cpa3
Pf4
Gstm5
Gpc3
Slc24a3
Fzr
Phf10
1700123O20Rik
Arid3b
Ado ra3
St3gal5
Mapk13
Gpr84
C130050O18Rik
Rab39
Kynu
Gpnmb
Cd86
Ak8
Fam129a
Tmem154
Gm4788
Ppfibp2
Ripk2
1700026L06Rik
Gm1673
Unc119
Ednrb
Mical2
Asf1b
Stag3
Tirap
Gm962
Tmem63a
Bmx
Gpx3
Pparg
Olfm4
Fam83f
Raet1b
Armc3
Rusc2
Id2
Havcr2
Clec4n
Thbs1
Fam89a
Slc52a3
Rpl3l
Card10
Cldn1
Klra17
Sdk1
Stfa2l1
Plxnb3
Stfa3
Ttc39a
Crispld2
Hbb-y
Gm5416
Stfa2
2010005H15Rik
Arhgef11
Dhrs1
Gsdmd
Cryl1
Wdr1
Cln3
Fcgrt
Axl
Gng2
Tmem9b
Tcf19
Trpv2
Ctnnbip1
6330416G13Rik
Gm5483
Cdkn3
Aldh3a2
Leprot
Birc5
Coro1b
E14.5_MDP_FL_1
E14.5_MDP_FL_2
E14.5_MDP_FL_3
E14.5_MP_FL_1
E14.5_MP_FL_2
E14.5_MP_FL_3
E14.5_cMOP_FL_1
E14.5_cMOP_FL_2
E14.5_cMOP_FL_3
E14.5_Mono_Ly6CHi_FL_1
E14.5_Mono_Ly6CHi_FL_2
E14.5_Mono_Ly6CHi_FL_3
MDP_1
MDP_2
MDP_3
MDP_4
A2M_BM_cMOP_1
A2M_BM_cMOP_2
Adult_BM_Gr1_Hi_1
Adult_BM_Gr1_Hi_2
Adult_BM_Gr1_Hi_3
Adult_BM_Gr1_Hi_4

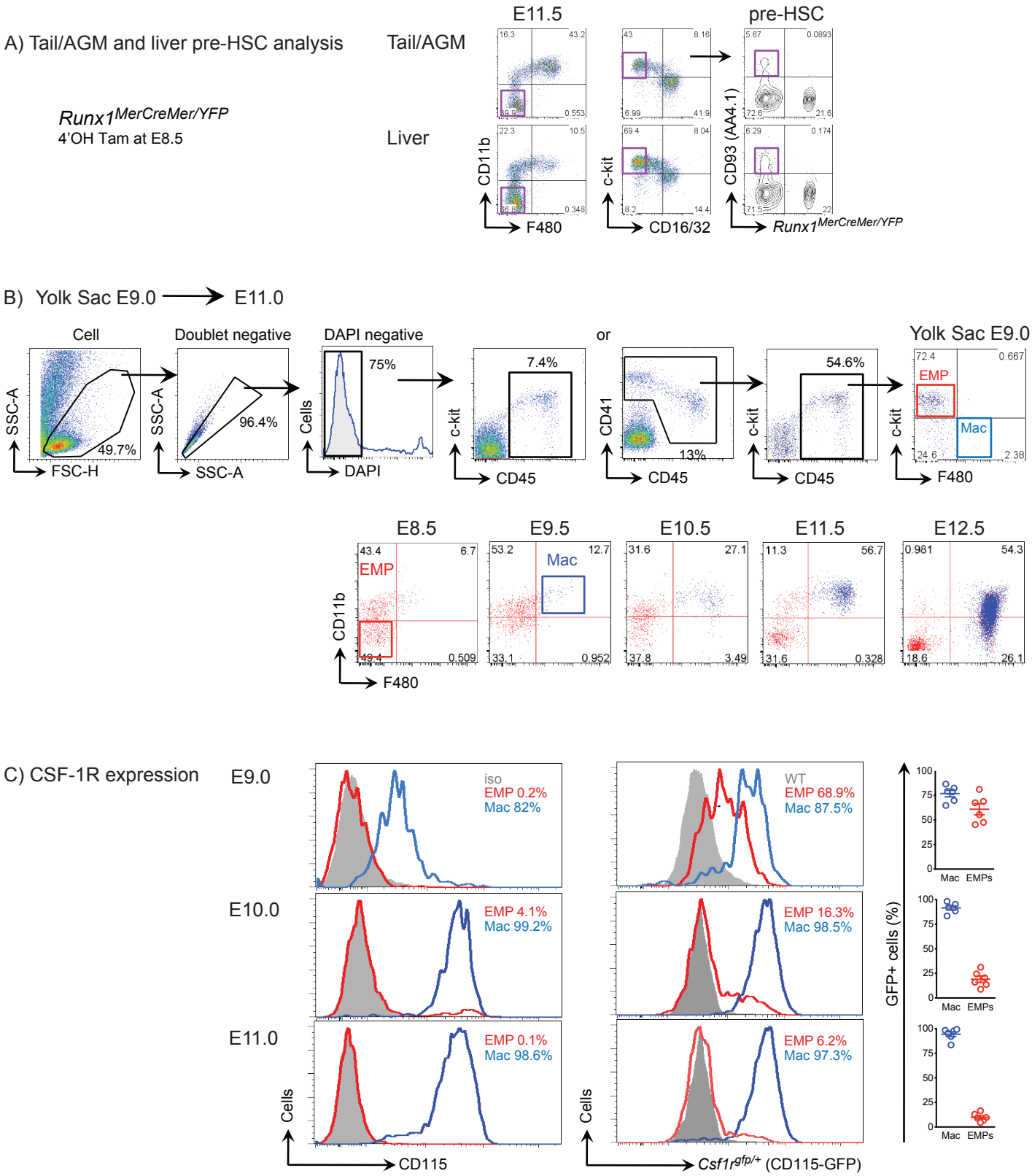

Figure S5: Characterization of Tail/AGM pre-HSC and Yolk sac EMP. *Related to Figure 5.*

(**A**) *Runx1*$^{MerCreMer/YFP}$ embryos were activated at E8.5 with 4'OHT and E11.5 tail/AGM and fetal liver were analyzed. Relative numbers of YFP$^+$ in c-Kit$^+$CD16/32$^-$CD93(AA4.1)$^+$ pre-HSC are shown. (**B**) Gating strategy to identify EMP and macrophages in the YS. (**C**) YS EMP and YS macrophages from E9.0 to E11.0 Macrophage Fas-Induced Apoptosis (MAFIA, *Csf1r*$^{gfp/+}$) CSF-1R reporter embryos were analyzed for CD115 (CSF-1R) surface expression (left) or mRNA expression (right). Each dot represents one embryo. Results are representative of two independent experiments.

	FL MDP signature		FL Ly6C$^-$MP signature		FL monocyte signature	
	scores	pVal	scores	pVal	scores	pVal
E14.5_FL_MDP_1	0.98	0	0.44	0.006	-0.45	0
E14.5_FL_MDP_2	1.00	0	0.46	0	0.00	0
E14.5_FL_MDP_3	1.00	0	0.53	2.00E-04	-0.59	0
E14.5_FL_MP_Ly6C$^-$1	0.36	0	1.00	0	-0.67	0
E14.5_FL_MP_Ly6C$^-$_2	0.59	0	0.98	0	-0.64	0
E14.5_FL_MP_Ly6C$^-$_3	0.36	0	0.98	0	-0.79	0
E14.5_FL_cMOP_1	-0.68	0	0.00	0.0247	0.32	0
E14.5_FL_cMOP_2	0.00	0.023	0.55	0	0.44	0
E14.5_FL_cMOP_3	-0.73	0	0.40	0.3402	0.42	0
E14.5_FL_Mono_Ly6C$^+$_1	-0.64	0	-0.90	0	1.00	0
E14.5_FL_Mono_Ly6C$^+$_2	-0.70	0	0.00	0.14	0.98	0
E14.5_FL_Mono_Ly6C$^+$_3	-0.71	0	-0.79	0.1054	0.98	0
Adult_BM_MDP_1	0.39	0	-0.64	0.0017	-0.95	0
Adult_BM_MDP_2	0.35	0	-0.85	7.00E-04	-0.89	0
Adult_BM_MDP_3	0.39	0	-0.62	0.0048	-1.00	0
Adult_BM_MDP_4	0.31	0	-0.65	0.0218	-0.91	0
Adult_BM_cMOP_1	-0.90	0	-0.70	0	-0.49	0
Adult_BM_cMOP_2	-0.87	0	-0.61	6.00E-04	-0.70	0
Adult_BM_Gr1_Hi_1	-1.00	0	-1.00	0	0.47	0
Adult_BM_Gr1_Hi_2	-0.93	0	-0.99	0	0.46	0
Adult_BM_Gr1_Hi_3	-0.95	0	-0.88	4.00E-04	0.43	0
Adult_BM_Gr1_Hi_4	-0.83	0.003	-0.98	0.0173	0.43	0

Table S1: CMAP score and p values of monocytes and monocyte precursors. *Related to Figure 4*

Each signature gene set was used as up and down-regulated genes to perform connectivity map (cMAP) (Lamb et al., 2006) analysis between myeloid progenitors derived from fetal liver or adult bone marrow. The p values were calculated through 1000 permutations. cMAP scores were scaled to the range from -1 to 1. *See Figure 4F and also Supplemental Methods.*

E14.5 FL MDP vs the rest Significant enrichment for E14.5 FL MDP				
Gene set	SIZE	ES	NES	FDR q-val
LYMPHOID	32	0.796789	2.201685	0
E14.5 FL Ly6C- MP vs the rest Significant enrichment for E14.5 FL Ly6C- MP				
Gene set	SIZE	ES	NES	FDR q-val
MKE	28	0.891902	2.421745	0
E14.5 FL mono vs the rest Significant enrichment for E14.5 FL mono				
Gene set	SIZE	ES	NES	FDR q-val
MYELOID	28	0.8221	2.230084	0
E14.5 FL Ly6C- MP vs E14.5 FL MDP Significant enrichment for E14.5 FL Ly6C- MP				
Gene set	SIZE	ES	NES	FDR q-val
MKE	28	0.876049	2.259854	0
MYELOID	28	0.748172	1.970503	0
E14.5 FL cMOP vs E14.5 FL MDP Significant enrichment for E14.5 FL cMOP				
Gene set	SIZE	ES	NES	FDR q-val
MYELOID	28	0.884294	2.212854	0
E14.5 FL cMOP vs E14.5 FL Ly6C- MP Significant enrichment in E14.5 FL cMOP				
Gene set	SIZE	ES	NES	FDR q-val
MYELOID	28	0.864416	2.375983	0
E14.5 FL mono vs E14.5 FL MOP Significant enrichment in E14.5 FL mono				
Gene set	SIZE	ES	NES	FDR q-val
MYELOID	28	0.805829	1.957614	5.60E-04

Table S3: GSEA reveals the loss of lymphoid and erythroid potential in cMoP and monocytes and their enrichment in myeloid genes. *Related to Figure 4H.*

Based on the three gene lists edited in *Table S1*, statistical enrichment was calculated for each population as followed: signature genes of FL MDP, FL MP Ly6C Lo, and FL monocytes, DEGs between FL MP Ly6C- vs FL MDP, DEGs between FL cMoP vs FL MDP, DEGs between FL cMoP vs FL MP Ly6C-, DEGs between FL monocytes vs FL cMoP. *See also Supplemental Methods.*

Supplemental Methods

Mice.

All experiments were performed on 6-12 week-old animals. *Runx1*$^{MerCreMer/WT}$ mice were obtained from Dr Igor Samokhvalov and bred with in-house with *Rosa*$^{R26R-EYFP/R26R-EYFP}$ mice as described in (Samokhvalov et al., 2007). *S100a4*$^{Cre/WT}$ [BALB/c-Tg(*S100a4*^{Cre})1Egn/YunkJ] were purchased from the Jackson Laboratory and bred in-house with *Rosa*$^{R26R-EYFP/R26R-EYFP}$ mice. Flt3-Switch mice were generated by crossing *Flt3*$^{Cre/WT}$ mice with R26$^{Tomato/GFP}$ [B6.129(Cg)-Gt(ROSA)26S or$^{tm4(ACTB-tdTomato,-EGFP)Luo}$/J] mice, and were bred at the University of California, Santa Cruz. *Csf1-r*$^{MerCreMer/WT}$ mice were purchased from the Jackson Laboratory and were crossed with the *Rosa*$^{R26R-EYFP/R26R-EYFP}$ reporter mice. Macrophage Fas-Induced Apoptosis (MAFIA) [C57BL/6-Tg(Csf1r-EGFP-NGFR/FKBP1A/TNFRSF6)2Bck/J] were purchased from the Jackson Laboratory. *Cx3cr1*$^{+/gfp}$ mice (Jung et al., 2000) and *Ccr2*$^{+/rfp}$ mice (Saederup et al., 2010) were maintained on a C57BL/6 background. C57BL/6 mice or heterozygous embryos were used as controls. Fucci-492 mice (Sakaue-Sawano et al., 2008) were purchased from the Riken BioResource Center (Ibaraki, Japan). Lysozyme-GFP mice were kindly provided by Dr. Thomas Graf of the Centre for Genomic Regulation, Barcelona, Spain (Faust et al., 2000). All experiments and procedures were approved by the Institutional Animal Care and Use Committee (IACUC), in accordance with the guidelines of the Agri-Food and Veterinary Authority (AVA) and the National Advisory Committee for Laboratory Animal Research (NACLAR) of Singapore.

Flow cytometry

Fluorochrome- or biotin- conjugated monoclonal antibodies (mAbs) specific for mouse CD11b (M1/70), CD45 (30F11), CD45.1 (A20), CD45.2 (104), CSF-1R (also called CD115; AFS98), Ly6C (AL21), Ly6G (1A8) CD3 (17A2), CD19 (1D3), NK1.1 (PK136), Ter119 (Ter119), Sca-1 (D7), CD93 (AA4.1), CD48 (hm48-1), CD150 (TC15-12F12.2), Flt3-biotin (A2F10), c-kit (also called CD117; 2B8), MerTK (108921), CD64 (X54-5/7.1) CD24 (M1/69), CD41 (MWReg30), CD16/32 (93)

CD34 (RAM34), Siglec-F (E50-2440), the corresponding isotype-matched controls and secondary reagents were purchased either from BD Biosciences or eBioscience. Anti-F4/80 (A3-1) mAb was purchased from Serotec (Raleigh, NC). Anti-F4/80 (A3-1) mAb was purchased from Serotec (Raleigh, NC)

Imaging procedures.

For cytospin preparations, corresponding myeloid progenitors were sorted using a FACS ARIA II (BD Biosciences) to achieve 98% purity. Purified cells were spun onto glass slides, dried for 20 minutes, stained for 1 minute in 0.3% Wright solution (Sigma), and rinsed in distilled water. Images were captured using a Nikon Eclipse E800 microscope (Nikon, Japan; Nikon Imaging Center, Chronos, Biopolis) at a 10 × 100-fold magnification.

Quantitative RT-PCR

Total RNA was extracted using the RNeasy Mini Kit (QIAGEN), and cDNA was synthesized with random hexamers and SuperScript III reverse transcriptase. For real-time PCR, cDNA products equivalent to RNA from 2,000 cells were amplified with a LightCycler_480 and SYBR Green I Master mix (Roche Diagnostics). The data were normalized to the amounts of gapdh RNA expression in each sample. The primers used for RT-PCR were as follows: *S100a4* FW: 5'-AGG AGC TAC TGA CCA GGG AG -3'; *S100a4* RV: 5'-CCT GTT GCT GTC CAA GTT GC-3'; *c-Myb* FW: 5'-TCA CCA GCA AGG TGC ATG AT-3'; *c-Myb* RV: 5'-TGC TGG AAG TGT AGA AAG A-3'; *Gapdh* FW: 5'-TGC GAC TTC AAC AGC AAC TC-3'; *Gapdh* RV: 5'-ATG TAG GCC ATG AGG TCC AC-3'

Gene array

Total RNA was extracted using the Life Technologies mirVana™ miRNA Isolation Kit (Ambion Inc, Austin, TX, USA). Agilent Bioanalyzer was used to assess RNA integrity and the RNA Integrity Number (RIN) was calculated. Only samples with a RIN ≥ 7 RNA were processed. Fifty ng of total RNA were used to prepare biotinylated cRNA using the TargetAmp™ Nano-g™ Biotin-aRNA Labeling Kit for the Illumina® System (Epicentre). Target cRNA was hybridized to the Illumina Mouse WG6 v2 Beadchips. Arrays were scanned using BeadArray Scanner 500GX at

the Biopolis Shared Facility, A*STAR, Singapore. Images were analyzed using the Illumina GenomeStudio Gene Expression v 1.9.0 software.

Microarray analysis

Microarray data was normalized by quantile normalization. Hierarchical clustering of samples was generated using Pearson's correlation and complete agglomeration method. Differentially expressed genes (DEGs) were selected by using Linear Models for Microarray Data (Limma) (Diboun et al., 2006) and a False Discovery Rate (FDR) cut-off of 0.05. Hierarchical clustering of monocytes and macrophages from fetal dermis and epidermis at E16.5 and E17.5 were used to select DEGs only expressed in fetal monocytes and not in macrophages (See below and **Figure 3F and Figure S4**). Hierarchical clustering of myeloid progenitors and monocytes, in fetal liver and adult bone marrow, indicated similar monocytes development between fetal liver and bone marrow. In order to identify differences between fetal and adult monocytes, Limma was used to select genes that are up or down-regulated in fetal monocytes compared to adult monocytes (**Figure 4E**). Bio-functions significantly enriched in these DEGs were identified by Ingenuity Pathway Analysis software (**Figure 4E**).

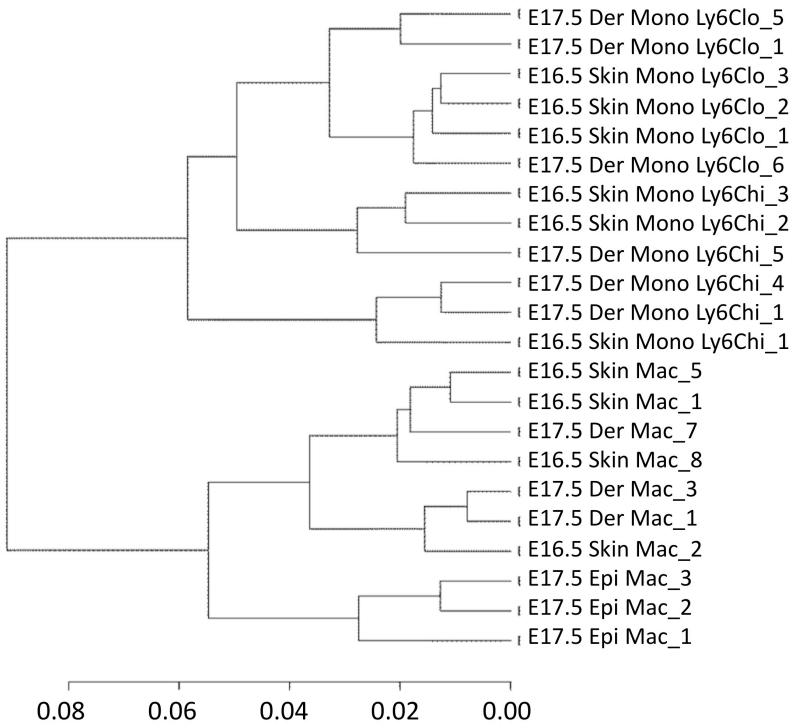

Hierarchical clustering of monocytes and macrophages at E16.5 and E17.5.

cMAP analysis

Signature genes of FL MDP, Ly6C$^-$MP and monocytes were identified using Limma to compare each myeloid progenitor and monocytes to each other (**Figure S4 and Figure 4F**). Each signature gene set was used as up and down-regulated genes to perform connectivity map (cMAP) (Lamb et al., 2006) analysis between myeloid progenitors derived from FL or adult bone marrow. The p values were calculated through 1000 permutations. cMAP scores were scaled to the range from -1 to 1. Cell types with positive cMAP score correlate with the corresponding cell type used as reference (Maximum score of 1) for cMAP analysis (See also **Table S1** for CMAP statistical data).

GSEA analysis

Three gene sets respectively termed Megakaryocytes/Erythocytes (MkE), Myeloid and Lymphoid were collected from (Boiers et al., 2013). Entrez gene IDs of these three gene sets are listed in **Table S2**. Gene set enrichment analysis (GSEA) was performed with the GSEA software (Subramanian et al., 2005) using the three gene sets for the following sets of signature genes: signature genes of FL MDP, FL Ly6C$^-$ MP and FL monocytes, DEGs between FL MP Ly6C$^-$ vs FL MDP, DEGs between FL cMoP vs FL MDP, DEGs between FL cMoP vs FL Ly6C$^-$ MP, DEGs between FL monocytes vs FL cMoP. See also **Table S3** for GSEA enrichment results.

Supplemental References

Boiers, C., Carrelha, J., Lutteropp, M., Luc, S., Green, J.C., Azzoni, E., Woll, P.S., Mead, A.J., Hultquist, A., Swiers, G.*, et al.* (2013). Lymphomyeloid contribution of an immune-restricted progenitor emerging prior to definitive hematopoietic stem cells. Cell stem cell *13*, 535-548.

Diboun, I., Wernisch, L., Orengo, C.A., and Koltzenburg, M. (2006). Microarray analysis after RNA amplification can detect pronounced differences in gene expression using limma. BMC genomics *7*, 252.

Faust, N., Varas, F., Kelly, L.M., Heck, S., and Graf, T. (2000). Insertion of enhanced green fluorescent protein into the lysozyme gene creates mice with green fluorescent granulocytes and macrophages. Blood *96*, 719-726.

Friedman, A.D. (2002). Transcriptional regulation of granulocyte and monocyte development. Oncogene *21*, 3377-3390.

Ginhoux, F., Greter, M., Leboeuf, M., Nandi, S., See, P., Gokhan, S., Mehler, M.F., Conway, S.J., Ng, L.G., Stanley, E.R., *et al.* (2010). Fate mapping analysis reveals that adult microglia derive from primitive macrophages. Science *330*, 841-845.
Jung, S., Aliberti, J., Graemmel, P., Sunshine, M.J., Kreutzberg, G.W., Sher, A., and Littman, D.R. (2000). Analysis of fractalkine receptor CX(3)CR1 function by targeted deletion and green fluorescent protein reporter gene insertion. Molecular and cellular biology *20*, 4106-4114.
Lamb, J., Crawford, E.D., Peck, D., Modell, J.W., Blat, I.C., Wrobel, M.J., Lerner, J., Brunet, J.P., Subramanian, A., Ross, K.N., *et al.* (2006). The Connectivity Map: using gene-expression signatures to connect small molecules, genes, and disease. Science *313*, 1929-1935.
Molawi, K., and Sieweke, M.H. (2013). Transcriptional control of macrophage identity, self-renewal, and function. Advances in immunology *120*, 269-300.
Saederup, N., Cardona, A.E., Croft, K., Mizutani, M., Cotleur, A.C., Tsou, C.L., Ransohoff, R.M., and Charo, I.F. (2010). Selective chemokine receptor usage by central nervous system myeloid cells in CCR2-red fluorescent protein knock-in mice. PloS one *5*, e13693.
Sakaue-Sawano, A., Kurokawa, H., Morimura, T., Hanyu, A., Hama, H., Osawa, H., Kashiwagi, S., Fukami, K., Miyata, T., Miyoshi, H., *et al.* (2008). Visualizing spatiotemporal dynamics of multicellular cell-cycle progression. Cell *132*, 487-498.
Samokhvalov, I.M., Samokhvalova, N.I., and Nishikawa, S. (2007). Cell tracing shows the contribution of the yolk sac to adult haematopoiesis. Nature *446*, 1056-1061.
Subramanian, A., Tamayo, P., Mootha, V.K., Mukherjee, S., Ebert, B.L., Gillette, M.A., Paulovich, A., Pomeroy, S.L., Golub, T.R., Lander, E.S., and Mesirov, J.P. (2005). Gene set enrichment analysis: a knowledge-based approach for interpreting genome-wide expression profiles. Proceedings of the National Academy of Sciences of the United States of America *102*, 15545-15550.